International Journal of Materials Science and Applications
2026, Vol. 15, No. 3, pp. 92–99
https://doi.org/10.11648/j.ijmsa.20261503.12

SciencePG
Science Publishing Group

Research Article

Synthesis of Chabazite Zeolite and Evaluation of Its Catalytic Property During the Esterification Reaction of Acetic Acid and Isoamyl Alcohol

Ferland Ngoro-Elenga[1, 2, *], Fernand Atipo Itoua Ngopoh[1], Longin Justin Clair Bonazaba Milandou[3], Prince Exauce Niama Nieme[1], Martin Tchoumou[1], Joseph-Marie Moutou[1]

[1]Laboratory of Inorganic and Applied Chemistry, Marien Ngouabi University, Brazzaville, Republic of Congo
[2]Geological and Mining Research Centre, Ministry of Mining Industries and Geology, Brazzaville, Republic of Congo
[3]Unit of Plant and Life Chemistry, Marien Ngouabi University, Brazzaville, Republic of Congo

Abstract

Chabazite is a microporous material widely studied due to its applications in heterogeneous catalysis. In this study, the authors synthesized a zeolite by the hydrothermal method at 125°C using tetrapropylammonium bromide as an organic template, which was removed by calcination at 800°C. The characterization of the synthesized product was carried out by X-ray diffraction, Fourier transform infrared spectroscopy, X-ray fluorescence, scanning electron microscopy coupled with energy-dispersive spectroscopy. X-ray diffraction showed the presence of a crystalline phase consisting of chabazite crystallizing in the rhombohedral lattice with lattice parameters a = 9.4250 Å and α = 94.060°. Fourier transform infrared spectroscopy revealed absorption bands located between 400 – 1000 cm^{-1}, characteristic of zeolites. X-ray fluorescence highlighted the aluminosilicate nature with a Si/Al ratio of 4.5 for the synthesized product. The SEM coupled with EDS revealed the uniformity of the product, a hexagonal morphology or the symmetrical facets characteristic of rhombohedral symmetry. The protonated form of the synthesized zeolite, obtained by ion exchange, was used as a catalyst for the synthesis of isoamyl acetate with a yield of the impure product of 79.03%; this yield being close to the same product obtained (84.76%) from the same reaction catalyzed by sulfuric acid. The UV-visible spectral data validated the synthesis products.

Keywords

Zeolite, Chabazite, Catalysis, Isoamyl Acetate, Esterification

1. Introduction

Zeolites are aluminosilicates of general formula $M_{x/n}(AlO_2)_x(SiO_2)_y.mH_2O$ where M is a metal cation of valence n and m is the number of water molecules of hydration. Their crystalline structure consists of a three-dimensional arrangement of SiO_4 and AlO_4- tetrahedra, linked at their vertices by oxygen atoms to form primary building units and ex-

*Correspondence: Ferland Ngoro-Elenga (ferland.ngoro-elenga@umng.cg)

Received: 20 March 2026; **Accepted:** 27 April 2026; **Published:** 16 May 2026

tended frameworks composed of identical blocks. The negative charge of zeolites results from the substitution of tetravalent silicon by trivalent aluminum. Since the covalent zeolite framework is anionic, charge-compensating cations M^{n+} ensure the electroneutrality of the solid [1-3]. These microporous solids are characterized by the presence of channels and/or cavities that communicate with the exterior. Zeolites can be natural or synthetic. Among the most well-known zeolites are analcime, mordenite, chabazite, ZSM-5, clinoptilolite, and stilbite. Due to their exceptional properties and excellent hydrothermal stability, zeolites can be used in ion exchange, adsorption, and catalysis [4-12]. Depending on the channel structure and pore size, zeolites can act as solid acid catalysts for chemical reactions such as esterification. Typically, esterification reactions are catalyzed by homogeneous mineral acids such as sulfuric acid or phosphoric acid [13, 14]. These homogeneous systems have several drawbacks, including corrosivity and toxicity, and are decomposed or removed by hydrolysis at the end of the reaction [13, 15]. The use of heterogeneous solid acid catalysts offers an alternative for acid-mediated organic syntheses, as they are easily separable and recoverable at the end of the reaction, with the possibility of reuse in multiple cycles [16-19]. Since its synthesis by Mobil in 1972, ZSM-5 remains the most widely used zeolite in catalysis. However, the catalytic performance of other zeolites, notably chabazite, has also been demonstrated [20, 21]. Indeed, chabazite can be synthesized either without an organic agent [22] or with an organic agent [23]. Several studies have revealed the use of tetrapropyl ammonium bromide (TPABr) or tetrapropyl ammonium hydroxide (TPAOH) in the synthesis of ZSM-5 [24-28], but no studies were found in the literature on the synthesis of chabazite using TPABr as an organic agent. Isoamyl acetate, being one of the most important esters used in the food industry due to its characteristic banana flavor [29], requires a catalyst for its synthesis. Thus, the general objectives of this study are to synthesize chabazite zeolite using TPABr as an organic agent and to evaluate the catalytic capacity of its protonated form in the esterification reaction of acetic acid and isoamyl alcohol.

2. Materials and Methods

2.1. Hydrothermal Synthesis of Chabazite Zeolite

In a beaker containing 5 mL of an aqueous sodium hydroxide solution 0.034 g/mL (Sigma-Aldrich), 0.66 g of $NaAlO_2$ (Strem Chemicals) was dissolved. After 5 minutes of stirring, 3 g of tetrapropylammonium bromide (Sigma-Aldrich) and 15 mL of Na_2SiO_3 (ALM International) were added to the reaction medium to form an aluminosilicate gel. After 20 h of aging, the gel was transferred into a Teflon container and placed in an autoclave, which was then heated at 125°C in an oven for 5 days. After crystallization, the resulting solid was recovered and washed with distilled water until reaching neutral pH. The product obtained was filtered and air-dried for 48 hours, then calcined in a furnace at gradually increasing temperatures for 4 days. On the first day, the product was heated from 25 to 500°C for 3 hours and maintained at 500°C for 1 hour. This operation was repeated for 4 days. However, on the fourth day, the heating was continued from 500 to 800°C for 4 hours and then maintained at 800°C for 2 hours.

2.2. Characterization Methods of the Synthesized Zeolite

X-ray diffraction was performed on a Panalytical X'Pert^3 powder diffractometer using a copper anticathode with wavelength $\lambda = 1.541$ Å. Phase identification was carried out using QualX software and the PowCod database. Fourier transform infrared (FTIR) spectroscopy was carried out on a Thermo Scientific Nicolet iS50 spectrometer scanning from 500 to 4000 cm^{-1}. Elemental composition was determined using Thermo Fisher Scientific XRF spectrometer. Morphology and local chemical composition were studied using a Regulus series scanning electron microscope coupled with energy-dispersive spectroscopy. Data processing and analysis were performed using Origin Pro 2024 sofware.

2.3. Activation of the Synthesized Zeolite

0.5 g of the synthesized product was introduced into a flask containing 50 mL of NaCl solution (1 M). The reaction medium was stirred gently for 24 hours at room temperature. After filtration and air-drying, the obtained product was treated with a NH_4Cl solution (1 M) under reflux at 60°C for 2 hours, filtered, and air-dried. The solid obtained was calcined at 400°C for 4 hours to obtain the protonated form of the material.

2.4. Synthesis of Isoamyl Acetate

The synthetic pathway is as described by reference [30]. In a round-bottom flask (100 mL), 7 mL of isoamyl alcohol, 10 mL of acetic acid, and the catalyst (0.12 g of activated zeolite or 1 mL of sulfuric acid) were successively introduced. The reaction mixture was subjected to magnetic stirring and refluxed at 70°C for 1 h in a water bath. After cooling, the mixture was transferred into a beaker containing approximately 150 g of ice. The organic phase was extracted with dichloromethane (2 × 25 mL), then washed successively with 50 mL of a sodium bicarbonate solution (10%) and 50 mL of distilled water. The impure esterification products obtained from both sulfuric acid and synthesized zeolite catalysis, along with pure acetic acid, were analyzed using a UV–Visible spectrophotometer (JENWAY 720). The wavelength range for analysis was set between 198 and 650 nm. Data were processed using Origin Pro 2024 software.

3. Results and Discussion

3.1. Characterization of the Synthesized Zeolite

The analysis results of the synthesized zeolite are presented in Figures 1 to 7.

Figure 1 shows the XRD pattern of the synthesized zeolite. This spectrum highlights the predominance of the Na-chabazite (card COD 00-901-4093, Trigonal, R-3m, a = 9.4250 Å, α = 94.060°), characterized by peaks located at 2θ (°) = 13.9, 21.8, 24.02; 27.9, 30.5 and 35.6 [31]. The FTIR spectrum of the synthesized product, shown in Figure 2, exhibits main bands located between 400 and 1000 cm^{-1}. The intense band at 961 cm^{-1} and the less intense ones at 714, 638, 575 and 544 cm^{-1} can be attributed to the internal vibrations of TO_4 tetrahedra (T = Si, Al) of the zeolitic framework. The absorption band at 961 cm^{-1} was assigned to the asymmetric stretching vibration, whereas the band at 714 cm^{-1} was associated with the symmetric stretching of Si–O–Si or Si–O–Al bridges in the tetrahedral framework. Additional bands at 638.07, 575.16 cm^{-1} were attributed to the bending vibrations of TO_4 groups, which may be associated with double four- or six-membered rings (D4R or D6R) [32-35].

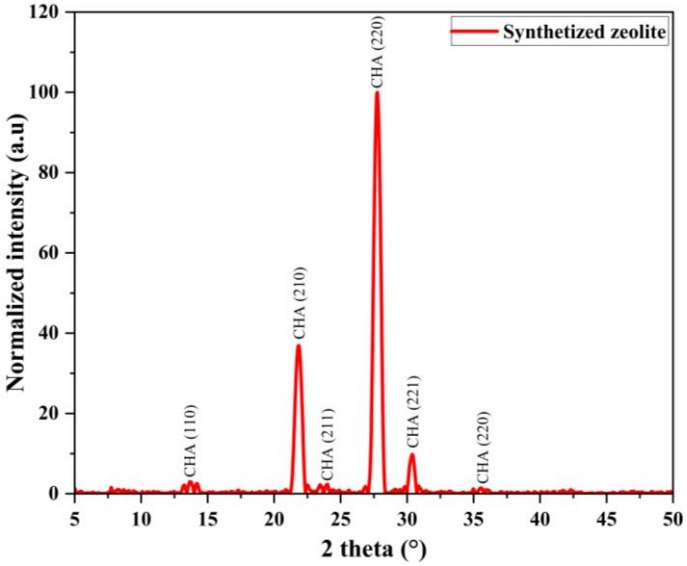

Figure 1. *XRD pattern of the synthesized zeolite.*

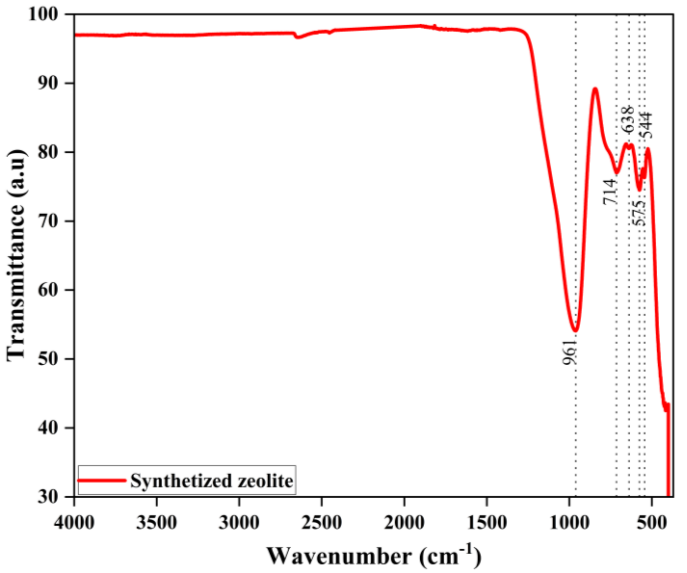

Figure 2. *FTIR spectrum of the synthesized zeolite.*

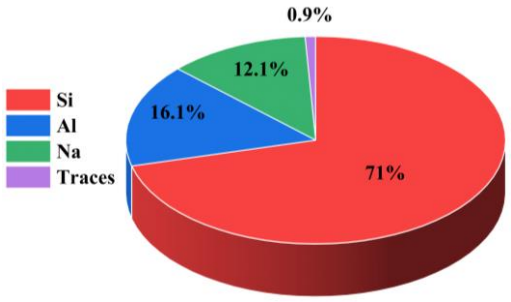

Figure 3. *Percentage of element.*

Figures 3 and 4 show, by X-ray fluorescence, the elemental and oxide composition of the synthesized compound. The analysis indicates Si contents of 70.97% or SiO_2 (69.08%) and Al contents of 16.09% or Al_2O_3 (17.66%). The percentages of Na element or Na_2O oxide are also significant, with values of 12.05% and 12.83%, respectively. The high contents of silicon (Si) or silicon oxide (SiO_2) and aluminum (Al) or aluminum oxide (Al_2O_3) indicate that the synthesized product is an aluminosilicate. The Si/Al ratio of 4.5 further confirms that the synthesized compound is a chabazite [36].

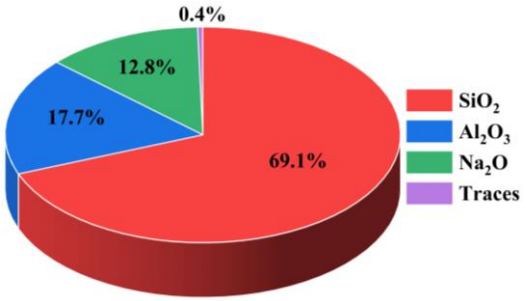

Figure 4. *Percentage of oxide.*

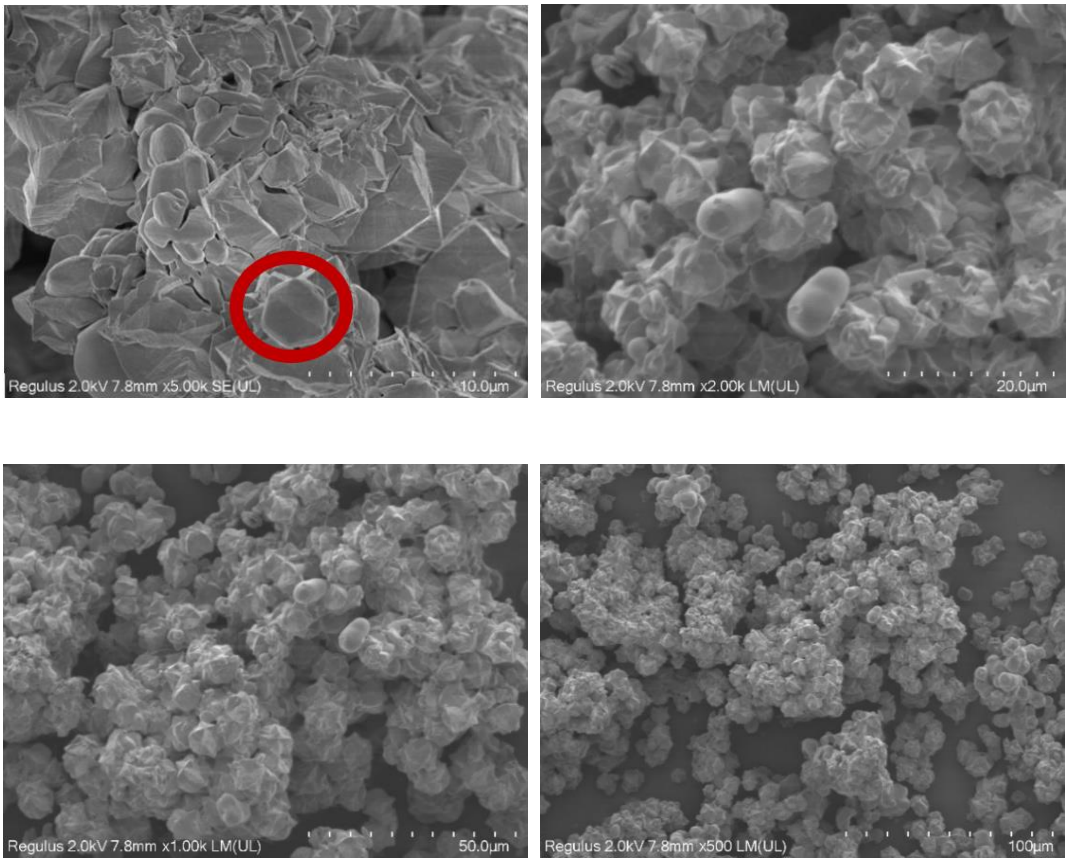

Figure 5. *Scanning electron micrographs of the synthesized zeolite.*

The scanning electron micrographs, shown in Figure 5, reveal the morphology and structure of the crystals of the synthesized product. The image at 10 µm indicate that the crystals exhibit the appearance of truncated hexagonal prisms or symmetric facets characteristic of rhombohedral symmetry. The rhombohedral form has also been reported by [37].

Figures 6 and 7 present the SEM/EDS results of the synthesized compound. Figure 6 shows that elemental analyses were performed on two regions of the product. The EDS spectra of these two regions (Figures 7 and 8) display the following results: region 1 (Al = 7.69%; Si = 19.91%) and region 2 (Al = 7.96%; Si = 19.90%), demonstrating the homogeneity of the obtained powder [38]. This analysis further confirms the aluminosilicate nature of the compound, with a predominance of silicon.

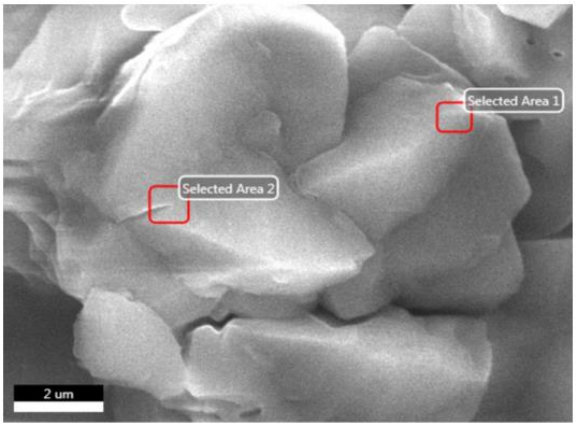

Figure 6. SEM images of the targeted zones.

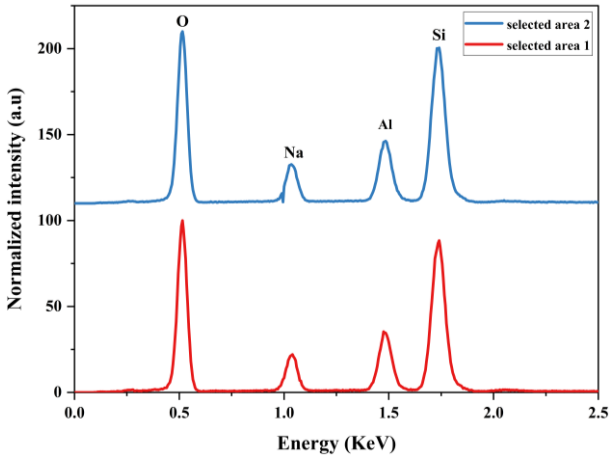

Figure 7. EDS spectrum of the synthesized product.

3.2. Characterization of the Esterification Products

Figure 8 shows the UV-Visible spectra of acetic acid and of the products obtained from esterification catalyzed by sulfuric acid and H-chabazite. Observation of the UV-Visible spectra of the esterification products revealed two absorption regions: the first band absorbing between 198 and 233 nm, and the second between 233 and 318 nm, with maximum absorption wavelengths at 213 and 271 nm, respectively. A similarity or overlap is observed between the spectra of the esterification products obtained with sulfuric acid and with H-chabazite. Based on the expected compounds or functional groups formed in this reaction, these bands correspond to the n→π* transitions of the C=O carbonyl groups of the carboxylic acid used (213 nm) and of the esters formed (271 nm) in this catalytic process [39, 40]. This indicates that the reaction product was not pure, as it exhibited characteristic bands of both the carbonyl groups of acetic acid (excess reactant in the medium) and those of the ester formed, with a bathochromic shift of the C=O group from acetic acid to the ester [39, 41]. These spectral data confirm the formation of isoamyl acetate within 1 hour of this esterification reaction catalyzed by H-chabazite. The yield of this impure product was 79.03%, which is comparable to that of the same impure liquid obtained (84.76%) from the reaction catalyzed by sulfuric acid. These results also suggest that H-chabazite is a more suitable catalyst for this reaction, as it is a recoverable solid and is likely to be less toxic and less corrosive than sulfuric acid.

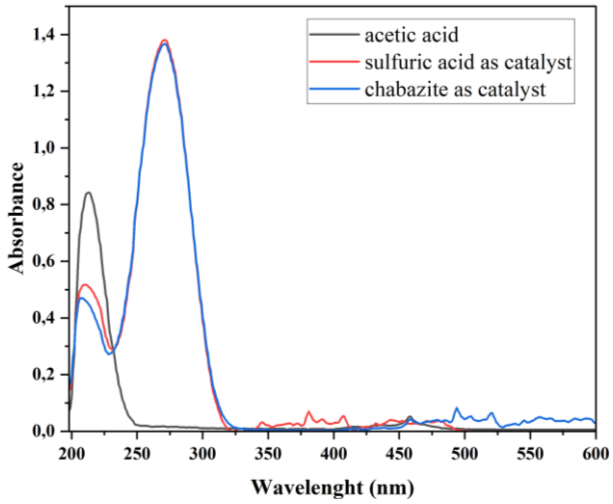

Figure 8. UV-vis spectra of acetic acid and of the esterification products.

4. Conclusion

The objectives of this work were to synthesize and characterize a chabazite-type zeolite and to evaluate its catalytic performance in the esterification of acetic acid and isoamyl alcohol. The analyses of the synthesized zeolite confirmed the presence of chabazite by X-ray diffraction, as well as characteristic zeolitic bands between 400 and 1000 cm^{-1} in Fourier-transform infrared spectroscopy. They also revealed the aluminosilicate nature of the product, with a Si/Al ratio of 4.5, indicating the presence of chabazite in the XRF analysis. SEM coupled with EDS confirmed the hexagonal prismatic morphology and the uniformity of the powder. The obtained zeolite was activated and used as a catalyst for the synthesis of isoamyl acetate, achieving a yield of 79.03% for the impure product, which is comparable to the yield of the same product obtained (84.76%) from the reaction catalyzed by sulfuric acid. The UV–visible absorption spectra of the esterification products were identical. The protonated form of the synthesized chabazite could therefore serve as a promising substitute for conventional catalysts used in esterification reactions.

Abbreviations

XRD	X-ray Diffraction
XRF	X-ray Fluorescence
FTIR	Fourier Transform Spectroscopy
SEM	Scanning Electron Microscopy

EDS Energy Dispersive Spectroscopy

Acknowledgments

The authors gratefully acknowledge the technical and administrative support of the Geological and Mining Research Centre (CRGM), Republic of Congo, through its Director General.

Author Contributions

Ferland Ngoro-Elenga: Conceptualization, Data curation, Methodology, Writing – original draft, Writing – review & editing

Fernand Atipo Itoua Ngopoh: Formal Analysis, Writing – review & editing

Longin Justin Clair Bonazaba Milandou: Formal Analysis, Writing – review & editing

Prince Exauce Niama Nieme: Methodology

Martin Tchoumou: Supervision, Validation

Joseph-Marie Moutou: Supervision, Validation

Funding

This research received no external funding.

Data Availability Statement

All data generated or analyzed during this study are including in the published article.

Conflicts of Interest

The authors declare no conflicts of interest.

References

[1] Baerlocher C., McCusker L. B., Olsen D. H. (2007). Atlas of zeolite framework type. 6th revised edition. Elsevier, Amsterdam, 398 p.

[2] Mortier W. J. (1982). Compilation of extra framework sites in zeolites. Butterworth Sientific Limited, London, 67 p.

[3] Abdoulaye A., Konaté M., Harouna M., Yahaya M., Rumori P., Palomino G. T. (2007). Caractérisation des analcimolites du bassin de Tim Mersoï (Nord du Niger) par diffraction des rayons X. C. R. Chimie 10, 546 – 551. https://doi.org/10.1016/j.crci.2007.02.002

[4] Ren L. M., Wu Q. M., Yang C. G., Zhu L. F., Li C. J., Zhang P. L., Zhang H. Y., Meng X. J., Xiao F. S. (2012). Solvent-free synthesis of zeolites from solid raw materials. Journal of the American Chemical Society, 134, 15173 – 15176. https://doi.org/10.1021/ja3044954

[5] Zhang H., Samsudin I. B., Jaenicke S., Chuah G.-K. (2022). Zeolites in catalysis: substainable synthesis and impact on properties and application. Catalysis Science & Technology, 12, 6024. https://doi.org/10.1039/d2cy01325h

[6] He J., Liu Z., Yoneyama Y., Nishiyama N., Tsubaki N. (2006). Multiple-Functional Capsule Catalysts: A Tailor-Made Confined Reaction Environment for the Direct Synthesis of Middle Isoparaffins from Syngas. Chemistry European Journal, 12, 8296 – 8304. https://doi.org/10.1002/chem.200501295

[7] Choi M., Na K., Kim J., Sakomoto Y., Terasaki O., Ryoo R. (2009). Stable single-unit-cell nanosheets of zeolite MFI as active and long-lived catalysts. Nature 461, 246 – 249. https://doi.org/10.1038/nature08288

[8] Xie B., Zhang H. Y., Yang C. G., Liu S. Y., Ren L. M., Zhang L., Meng X. J, Yilmaz B., Muller U., Xiao F. S. (2011). Seed-directed synthesis of zeolites with enhanced. performance in the absence of organic templates. Chemical Communications, 47, 3945-3947. https://doi.org/10.1039/C0CC05414C

[9] Chen X., Todorova T., Vimont A., Ruaux V., Qin Z., Gilson J. P., Valtchev V. (2014). In situ and post-synthesis control of physicochemical properties of FER-type crystals. Microporous and Mesoporous Materials, 200, 334-342. https://doi.org/10.1016/j.micromeso.2014.07.057

[10] Du Y., Zheng G., Wang J., Wang L., Wu J., Dai H. (2014). Microporous and Mesoporous Materials, 200, 27-34.

[11] Gao W., Amoo C. C., Zhang G., Javed M., Mazonde B., Lu C., Yang R., Xing C., Tsubaki N. (2019). Insight solvent-free synthesis of MOR zeolite and its laboratory scale production. Microporous and Mesoporous Materials, 280, 187-194. https://doi.org/10.1016/j.micromeso.2019.01.041

[12] Zhou L., Wang M., Yang S., Guo W., Pu X., He Y., Zhu J., Wang B., Zheng M., Liu S., Zhang Y. (2022). Facile synthesis of mesoporous ZSM-5 aided by sonication and application for VOCs capture. Ultrasonics Sonochemistry, 88, 106098. https://doi.org/10.1016/j.ultsonch.2022.106098

[13] Lodhi A., Maheria K. C. (2024). Zeolite-catalysed esterification of biomass-derived acids into high-value esters products: Toward sustainable chemistry. Catalysis communications, 187, 106883. https://doi.org/10.1016/j.catcom.2024.106883

[14] Pileids F. D., Titirici M. M. (2016). Luvulinic acid biorefineries: new challenges for efficient utilization of biomass. ChemSuschem 9, 562-582. https://doi.org/10.1002/cssc.201501405

[15] Maheria K. C., Lodhi A., Lankapati H., Krishna R. (2021). Solid acid-catalyzed esterification of levulinic acid for production of value-added chemicals. Catalysis for clean energy and environmental sustainability, Springer Cham, 345-382. https://doi.org/10.1007/978-3-030-65017-9_12

[16] Dal Pozzo D. M., Dos Santos J. A. A., Seabra Junior E., Santos R. F., Feiden A., Melegani de Souza S. N., Burgardt I. (2019). Free fatty acids esterification catalyzed by acid faujasite type zeolite. RSC Advances, 9, 4900-4907. https://doi.org/10.1039/C8RA10248A

[17] Fechete L., Wang Y., Védrine J. C. (2012). The past, present and future of heterogenous catalysis. Catalysis Today, 189, 2-27. https://doi.org/10.1016/j.cattod.2012.04.003

[18] Marso T. M. M., Kalpage C. S., Udugala-Ganehenege M. Y. (2017). Metal modified graphene oxide composite catalyst for production of biodiesel via pre-esterification of calophyllum inophyllum oil. Fuel, 199, 47-64. https://doi.org/10.1016/j.fuel.2017.01.004

[19] Mardhiah H. H., Ong H. C., Masjuki H. H., Lim S., Lee H. V. (2017). A review on latest developments and futurs prospects of heterogenous catalyst in biodiesel production from non-edible oils. Renewable and Substainable Energy Reviews, 67, 1225-1236. https://doi.org/10.1016/j.rser.2016.09.036

[20] Bull I., Moini A., Rai M. (2023). Chabazite zeolite catalysts having low silica to alumina ratios (US 11, 660, 585 B2, 2023.

[21] Van Speybroeck V., Hemelsoet K., De Wispelaere K., Qian Q., Van der Mynsbrugge J., De Sterck B., Weckhuysen B. M., Waroquier M. (2013). Mechanistic studies on chabazite-type methanol-to-olefin catalystes: insights time-resolved UV/Vis microspectroscopy combined with theoretical simulations. ChemCatChem, 5, 173-184. https://doi.org/10.1002/cctc.201200580

[22] Asmaly H. A., Elbager M. A., Ibrahim A. I., Nasser G. A. Abdelkreem S. S. E., Al-Suwaiyan, Elgzoly M. A. A. (2025). Synthesis of chabazite zeolite: a dual-function material for high-performance capture and para-nitrophenol removal from synthetic wastewater with comprehensive characterization and modeling. Chemical Engineering Science, 333, 121736. https://doi.org/10.1016/j.ces.2025.121736

[23] Dang L. V., Le S. T, Lobo R. F., Pham T. D. (2020). Hydrothermal synthesis of alkali-free chabazite zeolites. Journal of Porous Materials, 27, 1481-1489. https://doi.org/10.1007/s10934-020-00923-y

[24] Meng F., Wang Y., Wang S., Wang X., Wang S. (2017). Synthesis of ZSM-5 aggregates by a seed-induced method and catalytic performance in methanol-to-gasoline conversion. C. R. Chimie 20, 385-394. https://doi.org/10.1016/j.crci.2016.07.005

[25] Tao Y., Kanoh H., Kaneko K. (2003). ZSM-5 monolith of uniform mesoporous channels. Journal of American Chemistry Society, 125, 6044-6045. https://doi.org/10.1021/ja0299405

[26] Soualah A., Berkani M., Chater M. (2004). Synthèse et caractérisation des zéolithes de type ZSM-5. C. R. Chimie, 7, 713-720. https://doi.org/10.1016/j.crci.2004.04.005

[27] Dedecek J., Balgová V., Pashkova V., Klein P., Wichterlová B. (2012). Stnthesis of ZSM-5 zeolites with defined distribution of Al atoms in the framework and multinuclear MAS NMR analysis of the control of distribution. Chemistry Materials, 24, 3231-3239. https://doi.org/10.1021/cm301629a

[28] Li Y., Sun H., Feng R., Wang Y., Subhan F., Yan Z., Zhang Z., Liu Z. (2015). Synthesis of ZSM-5 zeolite from diatomite for fluid catalytic cracking (FCC) application. Appl Petrochem Res., 5, 347-353. https://doi.org/10.1007/s13203-015-0113-2

[29] Torres S., Baigorí M. D., Swathy S. L. Pandey A., Castro G. R. (2009). Enzymatic synthesis of banana flavour (isoamyl acetate) by *bacillus Licheniformis* S-89 esterase. Food Research International, 42, 454-460. https://doi.org/10.1016/j.foodres.2008.12.005

[30] Manzano Vela D. R. (2021). Esterification of artificial flavors. Synthesis of isoamyl acetate. International Journal of Innovative Science and Research Technology, 6(6), 1259-1263.

[31] Alberti A., Galli E., Vezzalini G., Passaglia E., Zanazzi P. F. (1982). Position of cations and water molecules in hydrated chabazite. Natural and Na-, Ca-, Sr- and K-exchanged chabazites. Zeolites, 2(4), 303-309. https://doi.org/10.1016/s0144-2449(82)80075-4

[32] Flaningen E. M., Khatami H., Szymanski H. A. (1971). Infrared Structural Studies of Zeolite Frameworks. In: Flanigen, E. M. and Sand, L. B., Ed., Molecular Sieve Zeolites, Advances in Chemistry 101, American Chemical Society, Washington DC, 201-229. https://doi.org/10.1021/ba-1971-0101.ch016

[33] Byrappa K., Suresh Kumar B. V. (2007). Characterization of zeolites by infrared spectroscopy. Asian Journal of chemistry, 19(6), 4933-4935.

[34] Król M., Mozgawa W., Jastrzebski W., Barezyk K. (2012). Application of IR spectra in the studies of zeolite from D4R and D6R structural groups. Microporous and Mesoporous Materials, 156, 181-188. https://doi.org/10.1016/j.micromeso.2012.02.040

[35] Farro N. W, Reyes W., Wendoza J. L., Veleva L., Quintana P., Azamar J. A., Aguilar D. (2023). Characterization by XRD and FTIR of zeolite A and zeolite X obtained from fly ash. Chemical Engineering Transaction, 99, 679-689. https://doi.org/10.3303/CET2399114

[36] Jha B., Singh, D. N. (2011). A review on synthesis, characterization and industrial application of flyash zeolites. *Journal of Materials Education, 33*(1–2), 65–132.

[37] Sato K., Sugimoto K., kikuchi K., Kyotani T., Kurato T. (2012). Development of practically available up-scaled hight-silicate CHA-type zeolite membranes for industrial purpose in dehydration of N-methyl pyrolidone solution. Journal of membrane science, 409-410, 82-95. https://doi.org/10.1016/j.memsci.2012.03.032

[38] González-Crisostomo J. C., Lopèz-Juárez R., Yocupicio-Gasciola R. I., Villanuera E., Zavala-Flores E., Petranosvskii V. (2022). Chabazite synthesis and its exchange with Ti, Zn, Cu, Ag and Au for efficient photocatalylic degradation of methylene blue. International Journal of Molecular Sciences, 23(3), 1-18. https://doi.org/10.3390/ijms23031730

[39] Skoog D. A, Holler F. J., Crouch S. R. (2017). Principles of instrumental analysis. 7th edition, Cengage Learning, Boston, United States, 959 p.

[40] Pavia D. L., Lampman G. M., Kriz G. S. (2001). Introduction to spectroscopy: A guide for Organic chemistry. 3rd edition, Brooks/Cole, Thomson Learning, Victoria, United States, p. 992.

[41] Sow I. S., Gelbcke M., Meyer F., Vandeput M., Marloye M., Basov S., Bael M. J. V., Berger G., Robeyns K., Hermans S., Yang D., V. Fontaine, Dufrasne F. (2023). Synthesis and biological activity of iron (II), iron (III), nickel (II), copper (II) and zinc (II) complexes of aliphatic hydroxamic acids. Journal of Coordination Chemistry, 76(1), 76–105. https://doi.org/10.1080/00958972.2023.2166407